A Search for Time-Dependent $B_s^0 - \overline{B_s^0}$ Oscillations Using Exclusively Reconstructed $D_s^{\pm}$ Mesons

Kenji Abe,[15] Koya Abe,[24] T. Abe,[21] I. Adam,[21] H. Akimoto,[21] D. Aston,[21] K.G. Baird,[11] C. Baltay,[30] H.R. Band,[29] T.L. Barklow,[21] J.M. Bauer,[12] G. Bellodi,[17] R. Berger,[21] G. Blaylock,[11] J.R. Bogart,[21] G.R. Bower,[21] J.E. Brau,[16] M. Breidenbach,[21] W.M. Bugg,[23] T.H. Burnett,[28] P.N. Burrows,[17] A. Calcaterra,[8] R. Cassell,[21] A. Chou,[21] H.O. Cohn,[23] J.A. Coller,[4] M.R. Convery,[21] R.F. Cowan,[13] G. Crawford,[21] C.J.S. Damerell,[19] M. Daoudi,[21] N. de Groot,[2] R. de Sangro,[8] D.N. Dong,[21] M. Doser,[21] R. Dubois,[21] I. Erofeeva,[14] V. Eschenburg,[12] S. Fahey,[5] D. Falciai,[8] J.P. Fernandez,[26] K. Flood,[11] R. Frey,[16] E.L. Hart,[23] K. Hasuko,[24] S.S. Hertzbach,[11] M.E. Huffer,[21] M. Iwasaki,[16] D.J. Jackson,[19] P. Jacques,[20] J.A. Jaros,[21] Z.Y. Jiang,[21] A.S. Johnson,[21] J.R. Johnson,[29] R. Kajikawa,[15] M. Kalelkar,[20] H.J. Kang,[20] R.R. Kofler,[11] R.S. Kroeger,[12] M. Langston,[16] D.W.G. Leith,[21] V. Lia,[13] C. Lin,[11] G. Mancinelli,[20] S. Manly,[30] G. Mantovani,[18] T.W. Markiewicz,[21] T. Maruyama,[21] A.K. McKemey,[3] R. Messner,[21] K.C. Moffeit,[21] T.B. Moore,[11] M. Morii,[21] D. Muller,[21] V. Murzin,[14] S. Narita,[24] U. Nauenberg,[5] H. Neal,[30] G. Nesom,[17] N. Oishi,[15] D. Onoprienko,[23] R.S. Panvini,[27] C.H. Park,[22] I. Peruzzi,[8] M. Piccolo,[8] L. Piemontese,[7] R.J. Plano,[20] R. Prepost,[29] C.Y. Prescott,[21] B.N. Ratcliff,[21] J. Reidy,[12] P.L. Reinertsen,[26] L.S. Rochester,[21] P.C. Rowson,[21] J.J. Russell,[21] O.H. Saxton,[21] T. Schalk,[26] B.A. Schumm,[26] J. Schwiening,[21] V.V. Serbo,[21] G. Shapiro,[10] N.B. Sinev,[16] J.A. Snyder,[30] H. Staengle,[11] A. Stahl,[21] P. Stamer,[20] H. Steiner,[10] D. Su,[21] F. Suekane,[24] A. Sugiyama,[15] S. Suzuki,[15] M. Swartz,[9] F.E. Taylor,[13] J. Thom,[21] E. Torrence,[13] T. Usher,[21] J. Va'vra,[21] R. Verdier,[13] D.L. Wagner,[5] A.P. Waite,[21] S. Walston,[16] A.W. Weidemann,[23] E.R. Weiss,[28] J.S. Whitaker,[4] S.H. Williams,[21] S. Willocq,[11] R.J. Wilson,[6] W.J. Wisniewski,[21] J.L. Wittlin,[11] M. Woods,[21] T.R. Wright,[29] R.K. Yamamoto,[13] J. Yashima,[24] S.J. Yellin,[25] C.C. Young,[21] H. Yuta.[1]

(The SLD Collaboration)

[1] *Aomori University, Aomori , 030 Japan,*

[2] *University of Bristol, Bristol, United Kingdom,*

[3] *Brunel University, Uxbridge, Middlesex, UB8 3PH United Kingdom,*

[4] *Boston University, Boston, Massachusetts 02215,*

[5] *University of Colorado, Boulder, Colorado 80309,*

[6] *Colorado State University, Ft. Collins, Colorado 80523,*

[7] *INFN Sezione di Ferrara and Universita di Ferrara, I-44100 Ferrara, Italy,*

[8] *INFN Lab. Nazionali di Frascati, I-00044 Frascati, Italy,*

[9] *Johns Hopkins University, Baltimore, Maryland 21218-2686,*

[10] *Lawrence Berkeley Laboratory, University of California, Berkeley, California 94720,*

[11] *University of Massachusetts, Amherst, Massachusetts 01003,*

[12] *University of Mississippi, University, Mississippi 38677,*

[13] *Massachusetts Institute of Technology, Cambridge, Massachusetts 02139,*

[14] *Institute of Nuclear Physics, Moscow State University, 119899, Moscow Russia,*

[15] *Nagoya University, Chikusa-ku, Nagoya, 464 Japan,*

[16] *University of Oregon, Eugene, Oregon 97403,*

[17] *Oxford University, Oxford, OX1 3RH, United Kingdom,*

[18] *INFN Sezione di Perugia and Universita di Perugia, I-06100 Perugia, Italy,*

[19] *Rutherford Appleton Laboratory, Chilton, Didcot, Oxon OX11 0QX United Kingdom,*

[20] *Rutgers University, Piscataway, New Jersey 08855,*

[21] *Stanford Linear Accelerator Center, Stanford University, Stanford, California 94309,*

[22] *Soongsil University, Seoul, Korea 156-743,*

[23] *University of Tennessee, Knoxville, Tennessee 37996,*

[24] *Tohoku University, Sendai 980, Japan,*

[25] *University of California at Santa Barbara, Santa Barbara, California 93106,*

[26] *University of California at Santa Cruz, Santa Cruz, California 95064,*

[27] *Vanderbilt University, Nashville,Tennessee 37235,*

[28] *University of Washington, Seattle, Washington 98105,*

[29] *University of Wisconsin, Madison,Wisconsin 53706,*

[30] *Yale University, New Haven, Connecticut 06511.*

(Dated: July 22, 2002)

Abstract

A search for $B_s^0 - \overline{B_s^0}$ oscillations is performed using a sample of 400,000 hadronic Z^0 decays collected by the SLD experiment. The B_s^0 candidates are reconstructed in the $B_s^0 \to D_s^- X$ channel with $D_s^- \to \phi\pi^-$, $K^{*0}K^-$. The B_s^0 production flavor is determined using the large forward-backward asymmetry of polarized $Z^0 \to b\overline{b}$ decays and charge information in the hemisphere opposite that of the B_s^0 candidate. The decay flavor is tagged by the charge of the $D_s^\pm$. From a sample of 361 candidates with an average B_s^0 purity of 40%, we exclude the following values of the oscillation frequency: $\Delta m_s < 1.4$ ps^{-1} and $2.4 < \Delta m_s < 5.3$ ps^{-1} at the 95% confidence level.

PACS numbers: 13.20.He, 13.25.Hw, 14.40.Nd

I. INTRODUCTION

The primary motivation for studying neutral B meson oscillations is to measure the poorly known Cabibbo-Kobayashi-Maskawa (CKM) matrix element V_{td}. The B_d^0 oscillation frequency corresponds to the mass difference, Δm_d, between the physical eigenstates of the $B_d^0 - \overline{B_d^0}$ system, which is sensitive to $|V_{td}|$. Although Δm_d is measured to within 2.5% [1], theoretical uncertainties lead to a 20% uncertainty in the extraction of $|V_{td}|$ [2]. However, many uncertainties cancel in the ratio of mass differences in the B_d^0 and B_s^0 systems:

$$\frac{\Delta m_s}{\Delta m_d} = \frac{m_{B_s} f_{B_s}^2 B_{B_s}}{m_{B_d} f_{B_d}^2 B_{B_d}} \left|\frac{V_{ts}}{V_{td}}\right|^2 = (1.15 \pm 0.05)^2 \left|\frac{V_{ts}}{V_{td}}\right|^2, \quad (1)$$

where m_{B_d} and m_{B_s} are the B meson masses, f_{B_d} and f_{B_s} are the decay constants, and B_{B_d} and B_{B_s} are the "B-parameters". Using this formula, and assuming $|V_{ts}|$=$|V_{cb}|$, one can obtain a 5-10% theoretical uncertainty on $|V_{td}|$ [2, 3].

As yet, the B_s^0 oscillation frequency has not been measured. The published lower limit on Δm_s based on the combined results from ALEPH, DELPHI, OPAL and CDF is 13.1 ps^{-1} at the 95% confidence level [1]. In the context of the Standard Model, other measurements suggest that Δm_s may be just beyond this current limit [4].

This letter describes a study [5] of $B_s^0 - \overline{B_s^0}$ oscillations with the SLD experiment at SLAC. The measurement of B_s^0 mixing requires excellent decay time resolution in order to resolve the very fast oscillations. The technique described in this letter, using $B_s^0 \to D_s^- X$ decays [6] with $D_s^- \to \phi\pi^-$ or $K^{*0}K^-$, has excellent decay length resolution (the best of any B_s^0 analysis to date) and high purity (reconstruction of a D_s^- helps to discriminate against the prominent backgrounds from B^+ and B_d^0 mesons). This work also represents the first use of polarized beams in a search for B_s^0 mixing, which provide an effective new means of identifying the flavor of the B_s^0 meson at production.

II. APPARATUS AND EVENT SELECTION

This analysis is based on a data set of 400,000 events of the form $e^+e^- \to Z^0 \to hadrons$, collected from 1996 through 1998 by the SLD experiment. A detailed description of the experiment can be found elsewhere [7, 8]. The analysis uses charged tracks reconstructed in the Central Drift Chamber (CDC) and the pixel-based CCD vertex detector (VXD3). The momentum resolution from the combined CDC and VXD3 fit is determined to be

$\sigma_{p\perp}/p_\perp = 0.010 \oplus 0.0024 p_\perp$, where $p_\perp$ (in GeV/c) is the momentum of the track transverse to the beamline. The track impact parameter resolution in the transverse plane is $\sigma_{xy} = 8 \oplus 33/(p \sin^{3/2}\theta)$ μm and along the beam direction is $\sigma_z = 10 \oplus 33/(p \sin^{3/2}\theta)$ μm, where p (in GeV/c) is the track momentum and θ is the polar angle with respect to the electron beam. The tracking system is surrounded by the Cherenkov Ring Imaging Detector (CRID), a two-radiator system that allows good pion and kaon separation in the momentum range between 0.3 and 35 GeV/c.

The goal of the analysis is to measure or constrain the oscillation frequency. This is accomplished by using B_s^0 decay candidates that are flavor tagged at both production and decay, and by measuring the proper time of the decay through measurements of the B_s^0 decay length and energy. The decay time distributions of B mesons whose flavor at production and decay are different (the same), so called mixed (unmixed) events, are modulated by the oscillation frequency. A fit to these distributions constrains Δm_s.

Event reconstruction consists of four main steps: hadronic event selection, $Z^0 \to b\overline{b}$ event selection, D_s^- decay reconstruction, and partial reconstruction of B_s^0 decays. A hadronic event is identified as having at least seven charged tracks, a total energy of at least 18 GeV, and an event thrust axis satisfying $|cos\theta_{thrust}| < 0.85$. The thrust axis is calculated based on the energy clusters found in the liquid-argon calorimeter. The hadronic event selection removes essentially all dilepton events and other non-hadronic backgrounds. To enhance the fraction of $Z^0 \to b\overline{b}$ events in the sample, events are required to have at least one topologically reconstructed secondary vertex [9] with a vertex mass greater than 2 GeV in either hemisphere. The vertex mass calculation includes a correction for the missing momentum transverse to the B flight direction in order to partially account for missing particles. A neural network [10] is used to select a candidate secondary B vertex (if multiple topological secondary vertices exist) and its decay tracks. The resulting event sample is 97% pure $b\overline{b}$ with a single hemisphere b tagging efficiency of 54%.

The D_s^- is reconstructed in one of two modes, $D_s^- \to \phi\pi^-$ or $K^{*0}K^- \to K^+K^-\pi^-$. Oppositely charged tracks are first paired to form a ϕ (K^{*0}) candidate and a third track is then attached to form a D_s^- candidate. To maximize the discrimination between true D_s^- and combinatorial background events, kinematic information for the D_s^- candidate is fed into another neural network. In this case, the neural net inputs include CRID particle identification information for each of the three daughter tracks, the K^+K^- ($K^-\pi^+$) invariant

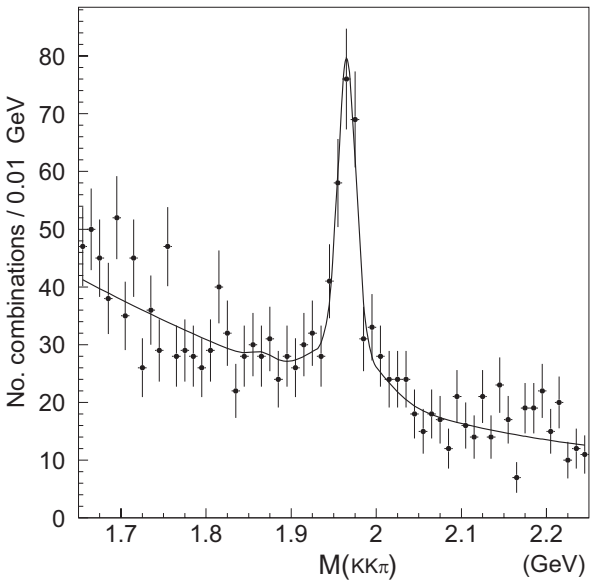

FIG. 1: Distribution of $KK\pi$ invariant mass for $\phi\pi$ and $K^{*0}K$ candidates combined, for the events that include a B_s^0 candidate vertex. The solid line shows a fit with the same functional form as is used in the likelihood function: two Gaussian distributions with common mean for the D_s signal, a single Gaussian for the D^+ contribution and a second-order polynomial for the background.

mass for ϕ (K^{*0}) candidates, the fit probability for the D_s^- decay vertex, the D_s^- decay length normalized by the decay length error, the total momentum of the D_s^-, the angle between the neutral meson (ϕ or K^{*0}) momentum in the D_s^- rest frame and the D_s^- flight direction, and the angle between the π^- or K^- from the D_s^- decay and the K^+ from the neutral meson decay in the rest frame of the neutral meson. The neural net cut that maximizes the sensitivity of the analysis to B_s^0 mixing is determined separately for each of the two D_s^- decay modes. The resulting $KK\pi$ mass distribution for both modes combined is shown in Figure 1.

The B_s^0 decay vertex is found by vertexing the virtual D_s^- track with other tracks in the hemisphere. The virtual D_s^- track is constructed by combining the 4-momenta of the three daughter tracks and constraining the parent D_s^- to pass through the decay vertex. The parent track error matrix is determined from propagation of the track measurement errors of the daughters. The B_s^0 vertex fit is accomplished in two steps: 1) identify an intersection of the virtual D_s^- track with another charged track in the same hemisphere to act as a seed for the B_s^0 decay vertex and 2) add other charged tracks to the seed vertex if they are more

consistent with coming from the B_s^0 decay than coming from the primary interaction point (IP). To find the seed, the D_s^- track is individually vertexed with each track (excluding D_s^- daughters) in the same hemisphere. The vertex that is farthest from the IP and upstream of the D_s^- (or consistent with being upstream within 5σ) and has a vertex fit χ^2 of less than 5 is chosen as the seed. In order to determine if another track should be added to the vertex, we examine two parameters: 1) the distance D from the IP to the seed vertex and 2) the distance L along the same direction from the IP to the point of closest approach of the track. If the ratio L/D is greater than 0.5 and the track forms a good vertex with the D_s^- (fit $\chi^2 \leq 5$), the track is added to the vertex. The latter condition is imposed to reject spurious tracks (often from a second charm decay if the B decayed to two charm particles) that do not point back to the B vertex. Only B decays for which the total charge of all associated tracks is Q=0 or ± 1 are kept for the $\phi\pi$ mode and those for which Q=0 are kept for the $K^{*0}K^-$ mode. The selected tracks are then vertexed together with the D_s^- to obtain the best estimate of the B decay position.

The IP location, needed to calculate the B_s^0 decay length, is determined from tracks that have vertex detector hits and extrapolate within 3σ of the beamline. The coordinates transverse to the beam are averaged over approximately 30 sequential hadronic Z^0 events, while the position along the beam is determined event-by-event. The resulting error in IP position is $3.5\mu m$ in the transverse plane and $17\mu m$ along the beam, the best resolution of any high energy physics collider. By making use of this well-determined beam spot, the very small beam size, and information from the high precision CCD vertex detector, this analysis has a unique sensitivity for measuring decay times of the B mesons.

An estimate of the B_s^0 decay length resolution is determined event-by-event according to the vertex fit and IP uncertainties, with correction factors applied for each particle decay hypothesis (B_s^0, B_d^0, B^+ or b-baryon) as determined from Monte Carlo simulation. The SLD Monte Carlo uses JETSET 7.4 with the B decay model tuned to CLEO and ARGUS data [11]. Parameterizing the decay length resolution as a sum of two Gaussians with normalizations of 0.6 (core) and 0.4 (tail), the estimated multiplicative correction factors for the B_s^0 signal events are 1.07 and 2.16 for the core and tail resolutions, respectively. The resulting average decay length resolution for the B_s^0 signal events is 50 μm (core) and 151 μm (tail).

The B meson boost is calculated from separate estimates for the charged and neutral

particle contributions to the total energy. The charged energy is determined by summing all the charged tracks associated with the B decay assuming the pion mass (except for the two kaons from the D_s^- decay). The neutral energy estimate uses five different techniques. The first four techniques are calorimeter-based and use various constraints (beam energy, jet energy, B_s^0 mass and calorimeter information) to estimate the neutral energy of the B meson [12]. The fifth technique is based only on the information from the charged decay tracks and the kinematics of the decay (B vertex axis, charged track momentum and B_s^0 mass constraint) [13]. The results from the five algorithms are then averaged, taking correlations into account, to obtain the total B energy. The resulting average boost resolution ($\frac{\sigma_{\gamma\beta}}{\gamma\beta}$) is represented by a sum of two Gaussians with widths (normalizations) of 8% and 18% (0.6 and 0.4) for the B_s^0 signal events.

Our final data sample includes 361 events within $\pm$40MeV of the D_s^- mass peak (Figure 1) with an average D_s^- purity of 48.1%. The composition of the D_s^- signal sample is calculated from the published branching ratio measurements with the relative reconstruction efficiencies of various decay modes taken from the Monte Carlo simulation. We estimate that the D_s^- signal peak consists of $B_s^0 \to D_s^\pm X$ (55.1%), $B_d^0 \to D_s^\pm X$ (22.4%), $B^+ \to D_s^\pm X$ (15.6%), b-baryon$\to D_s^\pm X$ (5.5%) and prompt $\overline{c} \to D_s^-$ (1.4%). For the hadronic B_s^0 decays, roughly 10% of the decays yield a wrong-sign D_s ($B_s^0 \to D_s^+ X$ instead of $B_s^0 \to D_s^- X$), due to $W^+ \to D_s^+$. Of the 361 B_s^0 candidates, 39 are semileptonic decay candidates ($B_s^0 \to D_s^- l^+ \nu X$). The fraction of wrong-sign D_s decays for the semileptonic modes is about 5%. These events have significantly higher B_s fraction and tagging purity than the hadronic decay sample, and therefore are parameterized separately.

III. TAGGING

The flavor of the B_s^0 at decay is determined by the charge of the D_s^-. A D_s^- is assumed to come from a B_s^0 and a D_s^+ is assumed to come from a $\overline{B_s^0}$. The B_s^0 flavor at production is obtained by exploiting the large forward-backward asymmetry in polarized $e^+ e^-_{L,R} \to Z^0 \to b\bar{b}$ decays. The differential cross section for the decay is given by

$$\frac{d\sigma(b)}{d\cos\theta} \propto (1 - A_e P_e)(1 + \cos^2\theta) + 2A_b(A_e - P_e)\cos\theta, \tag{2}$$

where the asymmetry parameter can be expressed in terms of vector and axial-vector couplings, $A_f = 2a_f v_f/(a_f^2 + v_f^2)$ and θ is defined as the angle between the outgoing fermion and the electron direction. The electron polarization is defined as $P_e = \frac{N(R)-N(L)}{N(R)+N(L)}$, where $N(R)$ ($N(L)$) is the number of right-handed (left-handed) electrons in a beam bunch. The outgoing b-quark is produced preferentially along the direction opposite to the spin of the Z^0 boson. Therefore, by knowing the polarization of the electron beam and the direction of the jet, the flavor of the primary quark in the jet can be inferred. The correct tag probability depends on the polar angle of the jet with respect to the incident electron beam direction and the electron beam polarization. The average electron beam polarization achieved during the run is about 73%. The resulting average correct tag probability is about 72%. In addition to the polarization tag, information from the hemisphere opposite to the reconstructed B_s^0 is used to improve the identification of the production flavor. A series of neural networks is used to combine momentum-weighted jet charge, vertex charge, dipole charge [8], lepton charge and kaon charge information. The purity of the opposite hemisphere charged tags has been calibrated from the data to be (70.4±0.8)%. Combining all available tags, the overall production flavor tag purity is (77.8±0.8)%. In the end, candidates for which the flavor of the B meson at decay is more than 50% likely to be different from the flavor at production are said to be 'mixed'.

IV. FITTING AND RESULTS

To determine the B_s^0 oscillation frequency, an unbinned likelihood function is used to describe the proper time distribution of mixed and unmixed events. For signal $B_s^0 \to D_s^{\pm} X$ events tagged as mixed (unmixed), the proper time distribution has the form,

$$P_{B_s}(\Delta m_s, t_{rec})^{mixed}_{unmixed} = \int_{-\infty}^{+\infty} \frac{1}{2\tau_{B_s}} \exp(-t/\tau_{B_s}) \; [\; 1 \mp (1-2\eta_{B_s}) \cos(\Delta m_s t)] \cdot \epsilon_{B_s}(t) \cdot G_{B_s}(t_{rec}, t) \cdot dt, \tag{3}$$

where t_{rec} is the reconstructed proper time, t is the true proper time, τ_{B_s} is the B_s^0 lifetime, $\epsilon_{B_s}(t)$ is the reconstruction efficiency and $G_{B_s}(t_{rec}, t)$ is the proper time resolution function for the B_s^0 events. The overall mistag probability is $\eta_{B_s} = \eta_i(1-\eta^f_{B_s}) + (1-\eta_i)\eta^f_{B_s}$, where η_i is the production flavor mistag probability and $\eta^f_{B_s}$ is the decay flavor mistag probability for the B_s^0 events. The efficiency and proper time resolution functions are derived from Monte

Carlo simulations. The Monte Carlo vertexing resolution is based on our understanding of the impact parameter resolution, which is carefully tuned to match the data. A comparison of decay length resolution between data and Monte Carlo using 3-prong τ decays shows good agreement. The proper time resolution is expressed in terms of decay length and boost resolutions (σ_L,$\sigma_{\gamma\beta}$) according to:

$$\sigma_t^{ij}(t) = \left[\left(\frac{\sigma_L^i}{\gamma\beta c} \right)^2 + \left(t \frac{\sigma_{\gamma\beta}^j}{\gamma\beta} \right)^2 \right]^{1/2} , \tag{4}$$

where the indices i, j =1 for core and 2 for tail resolution. Both σ_L and $\sigma_{\gamma\beta}$ are determined event-by-event. The decay length resolution σ_L depends on the B_s^0 vertex fit error matrix and IP uncertainties, and the boost resolution $\sigma_{\gamma\beta}$ is parameterized as a function of charged track energy in the decay. The decay time resolution function is comprised of four σ_t Gaussian distributions given by the various σ_L and $\sigma_{\gamma\beta}$ core-tail combinations.

The distribution for B_d^0 mesons, which are also subject to oscillations, is identical to equation 3 with B_s^0 subscripts replaced by B_d^0 subscripts. The terms for B^+ and b-baryon, which do not oscillate, are constructed in an analogous fashion, but with $\Delta m = 0$. The probability density function for the data sample has the form,

$$\begin{aligned} P \;=\; & f_{D_s} \left(\frac{f_{B_s}}{N_{B_s}} P_{B_s} + \frac{f_{B_d}}{N_{B_d}} P_{B_d} + \frac{f_{B^+}}{N_{B^+}} P_{B^+} + \frac{f_{b-bary}}{N_{b-bary}} P_{b-bary} + \frac{f_{cc}}{N_{cc}} P_{cc} \right) \\ & + \; [1 - f_{D_s}]\, P_{comb}. \end{aligned} \tag{5}$$

The fraction of D_s^- signal above the combinatorial $m_{KK\pi}$ background, f_{D_s}, is estimated from the previous D_s^- mass fit (Figure 1) as a function of $m_{KK\pi}$. The remaining fractions are calculated based on the measured branching ratios with reconstruction efficiencies taken from the Monte Carlo simulation. The function P_{cc} describes the prompt charm ($Z^0 \to c\bar{c}$) events, and is obtained from Monte Carlo simulation. The time distribution for the combinatorial events, P_{comb} is parameterized directly from the data using events in the D_s^- mass sidebands. The sideband regions are defined as: $1.7 < m_{KK\pi} < 1.8$ GeV (lower sideband) and $2.05 < m_{KK\pi} < 2.2$ GeV (upper sideband). The parameters N_i, are normalization constants, obtained by integrating the sum of P_{mixed} and $P_{unmixed}$ over all reconstructed proper time.

In the absence of a signal, the amplitude fit method [14] is used to set a limit on Δm_s. The amplitude fit is equivalent to a Fourier analysis, in which one searches for peaks in the frequency spectrum of oscillation. To perform an amplitude fit, the likelihood function is

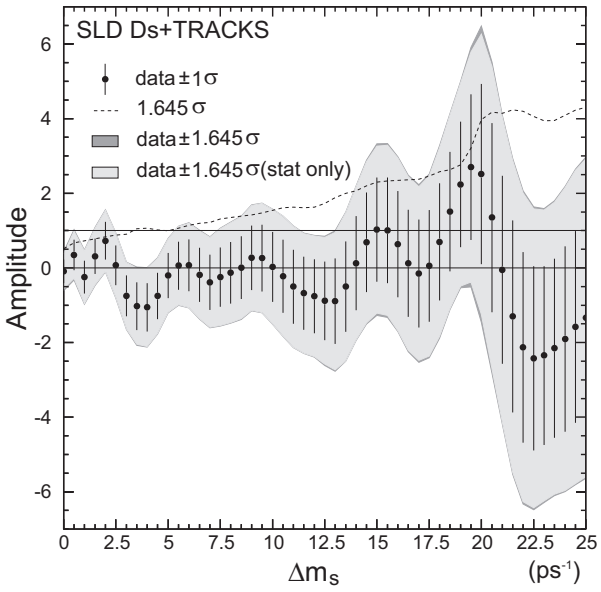

FIG. 2: Measured B_s^0 oscillation amplitude as a function of Δm_s. The light-grey (dark-grey) band shows the 90% confidence region obtained from statistical (total) uncertainties. Values of Δm_s for which the allowed band is below $A = 1.0$ are excluded at the one-sided 95% confidence level.

modified by replacing $\cos(\Delta m_s t)$ with $A \cdot \cos(\Delta m_s t)$. The amplitude A and its error σ_A are then measured at each assumed value of Δm_s. If mixing occurs at the chosen value of Δm_s, the fitted value of A should be consistent with unity. At values of Δm_s sufficiently far from the true mixing frequency, the fitted value of A should be close to zero, consistent with no oscillation. Values of Δm_s for which $A + 1.645\sigma_A \leq 1$ can be excluded at the 95% confidence level. We have tested this procedure on simulated data for Δm_s values of 4, 10, 17 and 270 ps^{-1} to verify that the amplitude fit behaves as expected in all cases.

The amplitude plot for this analysis is shown in Figure 2. There is no evidence for a significant signal anywhere in the plot, so we use the analysis to set a limit on Δm_s. The systematic errors on A are evaluated according to reference [14], all of which are negligible compared to the statistical errors. The systematics are dominated by uncertainties in a small reconstructed proper time bias (evaluated at 100% of the simulated correction, typically a few hundreths of a picosecond), in the production flavor tag (evaluated with ±0.8% uncertainty in the average tag probability and a reweighting of the shape of the distribution as a function of neural net output), in $f_{D_s^-}$ (as determined from the $KK\pi$ mass fit), and in the boost

TABLE I: B production fractions and various branching ratios assumed in the amplitude fit. The uncertainties for the branching ratios do not include the uncertainty from $\mathcal{B}(D_s \to \phi\pi)$.

Parameter	Value and Error	Ref.
$f(\overline{b} \to B_s^0)$	0.100 ± 0.012	[15]
$f(\overline{b} \to B_d^0, B^+)$	0.401 ± 0.010	[15]
$f(\overline{b} \to b-baryon)$	0.099 ± 0.017	[15]
$R_b \cdot f(b \to \overline{B_s^0}) \cdot \mathcal{B}(\overline{B_s^0} \to D_s^+ X) \cdot \mathcal{B}(D_s^+ \to \phi\pi^+)$	$(6.21^{+0.71}_{-0.78}) \times 10^{-4}$	[15, 16]
$f(b \to W^- \to D_s^-) \cdot \mathcal{B}(D_s^- \to \phi\pi^-)$	$(3.66 \pm 0.45) \times 10^{-3}$	[16]
$\mathcal{B}(B_d^0, B^+ \to D_s^\pm X) \cdot \mathcal{B}(D_s^- \to \phi\pi^-)$	$(3.71 \pm 0.28) \times 10^{-3}$	[15]
$\mathcal{B}(B_d^0, B^+ \to D_s^- X)/\mathcal{B}(B_d^0, B^+ \to D_s^\pm X)$	0.172 ± 0.083	[15]
$\mathcal{B}(\overline{c} \to D_s^-) \cdot \mathcal{B}(D_s^- \to \phi\pi^-)$	$(3.4 \pm 0.3) \times 10^{-3}$	[15]

resolution (10%). To a lesser extent, there are contributions from uncertainties in decay length resolution (7%) and branching fractions assumed in the fit. Uncertainties in particle lifetimes and in the B_d^0 oscillation frequency are completely negligible. The list of systematic errors is shown in Table II. The dark-grey band in Figure 2, barely visible at the edge of the light-grey band, shows the effect of adding the total systematic error to the calculations.

Based on the result of the amplitude fit, the values of the B_s^0 oscillation frequency excluded at the 95% confidence level are: $\Delta m_s < 1.4$ ps^{-1} and $2.4 < \Delta m_s < 5.3$ ps^{-1}.

V. CONCLUSIONS

In conclusion, we have performed a search for $B_s^0 - \overline{B_s^0}$ oscillations using 361 $B_s^0 \to D_s^- X$ candidate events with an average B_s^0 purity of 40%. The excluded values of oscillation frequency are: $\Delta m_s < 1.4$ ps^{-1} and $2.4 < \Delta m_s < 5.3$ ps^{-1} at the 95% confidence level. The analysis exploits the unique large polarized forward-backward asymmetry in $Z^0 \to b\bar{b}$ decays to enhance the production flavor tag. Combining the good production flavor tag and excellent proper time resolution, the analysis contributes to the world average at high Δm_s despite low statistics. Taken in conjunction with other published results, our result raises the 95% C.L. world limit on Δm_s from 13.1 ps^{-1} to 13.9 ps^{-1}.

TABLE II: Table of statistical and dominant systematic uncertainties for several Δm_s values.

Δm_s	10 ps^{-1}	15 ps^{-1}	20 ps^{-1}
Measured amplitude A	0.029	1.027	2.513
σ_A^{stat}	± 0.933	± 1.361	± 2.283
σ_A^{syst}	$^{+0.088}_{-0.084}$	$^{+0.312}_{-0.313}$	$^{+0.776}_{-0.789}$
$f(\overline{b} \to B_s^0)$	$^{+0.012}_{-0.012}$	$^{+0.021}_{-0.022}$	$^{+0.010}_{-0.011}$
$f(\overline{b} \to b-\text{baryon})$	$^{+0.004}_{-0.004}$	$^{+0.001}_{-0.001}$	$^{-0.019}_{+0.019}$
$R_b \cdot \mathcal{B}(b \to \overline{B_s^0}) \cdot \mathcal{B}(\overline{B_s^0} \to D_s^+ X)$	$^{-0.032}_{+0.043}$	$^{-0.040}_{+0.048}$	$^{-0.068}_{+0.068}$
$\mathcal{B}(b \to W^- \to D_s^-)$	$^{+0.013}_{-0.013}$	$^{+0.022}_{-0.022}$	$^{+0.010}_{-0.012}$
$\mathcal{B}(B_d^0, B^+ \to D_s^\pm X)$	$^{+0.013}_{-0.014}$	$^{+0.013}_{-0.014}$	$^{+0.042}_{-0.047}$
$\frac{\mathcal{B}(B_d^0, B^+ \to D_s^- X)}{\mathcal{B}(B_d^0, B^+ \to D_s^\pm X)}$	$^{+0.012}_{-0.013}$	$^{+0.058}_{-0.060}$	$^{+0.153}_{-0.156}$
$\mathcal{B}(\overline{c} \to D_s^-)$	$^{+0.003}_{-0.003}$	$^{+0.007}_{-0.007}$	$^{+0.011}_{-0.011}$
Decay length resolution	$^{+0.034}_{-0.036}$	$^{+0.015}_{-0.015}$	$^{+0.026}_{-0.045}$
Boost resolution	$^{+0.049}_{-0.048}$	$^{-0.052}_{+0.042}$	$^{-0.161}_{+0.140}$
f_{D_s}	$^{+0.019}_{-0.018}$	$^{+0.096}_{-0.096}$	$^{-0.090}_{+0.076}$
Average production flavor tag	$^{-0.029}_{+0.031}$	$^{-0.036}_{+0.036}$	$^{-0.051}_{+0.048}$
Production flavor tag shape	$^{-0.020}_{+0.018}$	$^{+0.008}_{-0.013}$	$^{+0.306}_{-0.318}$
Proper time offset	$^{+0.007}_{-0.007}$	$^{+0.278}_{-0.278}$	$^{+0.671}_{-0.671}$

Acknowledgments

We thank the personnel of the SLAC accelerator department and the technical staffs of our collaborating institutions for their outstanding efforts. This work was supported by the Department of Energy, the National Science Foundation, the Instituto Nazionale di Fisica of Italy, the Japan-US Cooperative Research Project on High Energy Physics, and the Science and Engineering Research Council of the United Kingdom.

[1] D.E. Groom *et al.*, The European Physical Journal **15** (2000) 1 and 2001 off-year partial update for the 2002 edition available on the PDG WWW pages (URL:http://pdg.lbl.gov/).

[2] C. W. Bernard, Nucl. Phys. B Proc. Suppl. **94**, 159 (2001).

[3] The small theoretical error in the ratio of B_s^0 to B_d^0 oscillation frequency quoted in the previous reference has recently been challenged. See A. S. Kronfeld and S. M. Ryan, arXiv:hep-ph/0206058.

[4] M. Ciuchini *et al.*, JHEP **0107**, 013 (2001).

[5] C-J. S. Lin, Ph.D. Dissertation, University of Massachusetts, Amherst, MA (2001), SLAC-R-584.

[6] Charge conjugate reactions are implied throughout this paper.

[7] SLD Design Report, SLAC Report 273 (1984).

[8] P. Rowson, D. Su, S.Willocq, Ann. Rev. Nucl. Part. Sci. **51**, 345 (2001).

[9] D. J. Jackson, Nucl. Inst. and Meth. **A388**, 247 (1997).

[10] K. Abe *et al.* [SLD Collaboration], SLAC-PUB-8542, July 2000.

[11] A. S. Chou, Ph. D. Dissertation, Stanford University, Stanford, CA (2001), SLAC-R-578.

[12] T. B. Moore, Ph.D. Dissertation, Yale University, New Haven, CT (1999).

[13] K. Abe *et al.* [SLD Collaboration], Phys. Rev. **D65**, 092006 (2002).

[14] H.G. Moser and A. Roussarie, Nucl. Inst. Meth., **A384**, 491 (1997).

[15] ALEPH, DELPHI, L3, OPAL, CDF, and SLD Collaborations, *Combined results on b-hadron production rates, lifetimes, oscillations and semileptonic decays*, CERN-EP-2000-096, SLAC-PUB-8492.

[16] D. Buskulic *et al.* [ALEPH Collaboration], Z. Phys. C **69**, 585 (1996).